

*Effect of Quartz/Mullite Blend Ceramic Additive on Improving  
Resistance to Acid of Sodium Silicate-activated Slag Cement*

**T. Sugama**  
Energy Science & Technology Department  
Brookhaven National Laboratory  
Upton, NY 11973-5000  
sugama@bnl.gov

**L.E. Brothers**  
Halliburton  
2600 S. 2<sup>nd</sup> Street  
Duncan, OK 73536  
Lance.Brothers@halliburton.com

**T.R. Van de Putte**  
CalEnergy Operating Corporation  
7030 Gentry Rd.  
Calipatria, CA 92233  
Todd.VandePutte@calenergy.com

June 2005

## **DISCLAIMER**

This report was prepared as an account of work sponsored by an agency of the United States Government. Neither the United States Government nor any agency thereof, nor any of their employees, nor any of their contractors, subcontractors, or their employees, makes any warranty, express or implied, or assumes any legal liability or responsibility for the accuracy, completeness, or any third party's use or the results of such use of any information, apparatus, product, or process disclosed, or represents that its use would not infringe privately owned rights. Reference herein to any specific commercial product, process, or service by trade name, trademark, manufacturer, or otherwise, does not necessarily constitute or imply its endorsement, recommendation, or favoring by the United States Government or any agency thereof or its contractors or subcontractors. The views and opinions of authors expressed herein do not necessarily state or reflect those of the United States Government or any agency thereof.

## **Abstract**

We evaluated the usefulness of manufactured quartz/mullite blend (MQMB) ceramic powder in increasing the resistance to acid of sodium silicate-activated slag (SSAS) cementitious material for geothermal wells. A 15-day exposure to 90° CO<sub>2</sub>-laden H<sub>2</sub>SO<sub>4</sub> revealed that the MQMB had high potential as an acid-resistant additive for SSAS cement. Two factors, the appropriate ratio of slag/MQMB and the autoclave temperature, contributed to better performance of MQMB-modified SSAS cement in abating its acid erosion. The most effective slag/MQMB ratio in minimizing the loss in weight by acid erosion was 70/30 by weight. For autoclave temperature, the loss in weight of 100°C-autoclaved cement was a less than 2 %, but at 300°C it was even lower. Before exposure to acid, the cement autoclaved at 100°C was essentially amorphous; increasing the temperature to 200°C led to the formation of crystalline analcime in the zeolitic mineral family during reactions between the mullite in MQMB and the Na from sodium silicate. In addition, at 300°C, crystal of calcium silicate hydrate (I) (CSH) was generated in reactions between the quartz in MQMB and the activated slag. These two crystalline phases (CSH and analcime) were responsible for densifying the autoclaved cement, conveying improved compressive strength and minimizing water permeability. The CSH was susceptible to reactions with H<sub>2</sub>SO<sub>4</sub>, forming two corrosion products, bassanite and ionized monosilicic acid. However, the uptake of ionized monosilicic acid by Mg dissociated from the activated slag resulted in the formation of lizardite as magnesium silicate hydrate. On the other hand, the analcime was barely susceptible to acid if at all. Thus, the excellent acid resistance of MQMB-modified SSAS cement was due to the combined phases of lizardite and analcime.

## Introduction

Our previous study of sodium silicate-activated slag (SSAS) cement as an acid-resistant cementitious material for geothermal wells focused on investigating the effectiveness of the crystalline hydrothermal reaction products yielded at temperatures between 100° and 300°C in inhibiting acid erosion [1]. The major phase of the SSAS cement after autoclaving at 100°C was calcium-silicate hydrate (CSH). Increasing temperature to 200°C led to the phase transformation of some CSH into tobermorite. At 300°C, the tobermorite → xonotlite phase transition took place, while most CSH was converted into well-formed tobermorite. When such cements were exposed to 90°C CO<sub>2</sub>-laden H<sub>2</sub>SO<sub>4</sub> (pH 1.1), we found that although the surfaces of all of them were vulnerable to attack by hot H<sub>2</sub>SO<sub>4</sub>, the 100°C-autoclaved specimens consisting of the CSH phase showed the lowest loss in weight, compared with that of the specimens autoclaved at 200° and 300°C. The reduction in the extent of erosion was due to the preferential reaction of the Ca-destitute CSH caused by the acid attack with Mg dissociated from the activated slag, thereby forming the lizardite phase. The newly arising Lizardites in the superficial layers of the acid-damaged cement not only retarded acid erosion, but also retained the integrity of the cementitious structure. In contrast, the Ca-depleted tobermorite and xonotlite phases did not react with Mg.

In trying to enhance further the resistance to acid of SSAS cement, our emphasis next was directed towards modifying its standard formulation with the Class F fly ash [2]. In that study, specimens were prepared by varying two parameters, the slag/fly ash ratio in the solid reactant and the SiO<sub>2</sub>/Na<sub>2</sub>O mol. ratio in the sodium silicate activator, before autoclaving them at 100°, 200°, and 300°C. The autoclaved cement specimens then were exposed to 90°C CO<sub>2</sub>-laden H<sub>2</sub>SO<sub>4</sub>. The tests showed that among the combination of these two parameters, the most effective one in retarding the acid erosion was a 50/50 slag/fly ash ratio and 2.50 SiO<sub>2</sub>/Na<sub>2</sub>O mol. ratio. The major contributor to minimizing acid erosion was the zeolite phases, such as analcium and Na-P type, formed by interactions between the mullite in fly ash and the Na ions liberated from the activator. Thus, the Class F fly ash offered an enhanced resistance to acid of SSAS cement.

Accordingly, the content of mullite in the Class F fly ash is very important in preparing the sodium silicate-activated slag/fly ash (SSASF) blend cement because of the

formation of the anti-acid zeolite phases. However, geothermal cementing operators have two concerns about the commercial Class F fly ash generated from coal-combustion power plants: One is its limited availability; and the other is the inconstancy of mullite content in each batch obtained from the supplier.

Recently, advanced technologies for ceramic synthesis have made it possible to manufacture an inexpensive fine ceramic powder consisting of the combinations of many different chemical ingredients. Thus, to deal with these problems of Class F fly ash, we decided to evaluate the usefulness of a synthesized granular ceramic additive made up with chemical constituents similar to that of Class F fly ash. This ceramic additive is manufactured under stringent quality control standards; currently it is being used as a lost circulation control material to quickly prevent losses of drilling fluids by bridging and sealing highly permeable pores and fractures.

Therefore, the objective in this study was to assess the effectiveness of the granular ceramic additive in reducing the vulnerability of SSAS cement to acid. The factors to be assessed included the compressive strength and water permeability of the autoclaved cements, and the identification of the phases formed in them. These data were integrated and correlated directly with acid erosion-related studies including weight changes, exploration of microstructure developed in the eroded cements' surfaces, and identification of reaction products yielded by the interactions between the acid and cement.

## **Experimental procedure**

### **Materials**

The granular ceramic additive known by the trade name "Pressure-seal Fine LCM" was supplied by TXI Energy Services Corp.; it had a specific gravity of 2.3 and a particle size of < 0.074 mm. The oxide composition of this additive consisted of 71wt% SiO<sub>2</sub>, 17wt% Al<sub>2</sub>O<sub>3</sub>, 4.5wt% Fe<sub>2</sub>O<sub>3</sub>, 2.2wt% CaO, 1.4wt% MgO, 0.85wt% TiO<sub>2</sub>, 0.2wt% P<sub>2</sub>O<sub>5</sub>, 0.45wt% Mn<sub>2</sub>O<sub>3</sub>, 0.7wt% Na<sub>2</sub>O, 1.1wt% K<sub>2</sub>O, and 0.55wt% SO<sub>3</sub>. X-ray diffraction (XRD) analysis revealed that this additive was comprised of two major crystalline phases, quartz and mullite, i.e., manufactured quartz/mullite blend (MQMB) ceramic additive. Lafarge North America Inc., supplied the ground granulated blastfurnace slag

cement. It had the following chemical constituents: 38.5wt% CaO, 35.2wt% SiO<sub>2</sub>, 12.6wt% Al<sub>2</sub>O<sub>3</sub>, 10.6wt% MgO, 1.1wt% Fe<sub>2</sub>O<sub>3</sub>, 0.4wt% TiO<sub>2</sub>, 0.9wt% S<sup>2-</sup>, and 0.3wt% SO<sub>3</sub>. The Blaine fineness of this cement was 5500 cm<sup>2</sup>/g. The sodium silicate aqueous solution under the commercial product name “STAR<sup>®</sup>” obtained from the PQ Corporation was used as the alkali activator. It was diluted with a deionized water to make a 20wt% activating solution. Test specimens were prepared in the following sequence. First, the slag cement was mixed with the MQMB additive in a twin shell dry blender to prepare the blended cements with slag/MQMB ratios of 90/10, 70/30, and 50/50 by weight. The unblended slag cement was used as the control. Second, the blended and unblended cements were mixed thoroughly with the activating solution at a solution-to-cement ratio of 0.65. Third, the cement slurry was cast into cylindrical molds, 30 mm in diameter and 65 mm long, and left to harden for at least 24 hours at room temperature. Finally, the hardened cement specimens were removed from the molds and autoclaved for 24 hours at 100°, 200°, or 300°C. The durability of autoclaved cements was tested by immersing them for 15 days in an H<sub>2</sub>SO<sub>4</sub> solution (pH 1.1) at 90°C containing 0.5 wt% sodium hydrogen carbonate (NaHCO<sub>3</sub>) as a source of ~ 3000 ppm CO<sub>2</sub>;  $H_2SO_4 + 2NaHCO_3 \rightarrow Na_2SO_4 + 2CO_2 + 2H_2O$ . This reaction was carried out in an autoclave to create an environment similar to that of a geothermal well, reflecting the incorporation of evolved CO<sub>2</sub> gases into the acid solution. To maintain the pH at 1.1, the H<sub>2</sub>SO<sub>4</sub> solution was replenished with a fresh solution every 5 days. The volume proportion of the cement specimens to the acid solution was 1 to 25.

## Measurements

The cement slurries for the compressive strength tests were cast in cylindrical molds (30 mm diam. x 65 mm length), and then the hardened cements were removed from the molds and cut to make specimens of 60 mm long; the result given is the average value from three specimens. Water permeability through the cylindrical cement specimens (50 mm diam. x 50 mm length) under a pressure of 202.65 kNm<sup>-2</sup> was determined by the Ruska liquid permeameter. The permeability measurements were made by determining the time necessary for a fixed amount of water at a given temperature to pass through the core under a given pressure gradient. X-ray powder diffraction (XRD)

was used to identify the phase compositions of the autoclaved cements before and after exposure in hot acid. The development and alternation of the microstructure in the cements after exposure was explored using scanning electron microscopy (SEM) coupled with energy-dispersive X-ray spectrometry (EDX).

## **Results and discussion**

### Compressive Strength

Figure 1 gives the changes in compressive strength of the cements made with the 100/0, 90/10, 70/30, and 50/50 slag/ MQMB ratios as a function of autoclave temperature. For the 100/0 ratio control cements (without the MQMB), autoclaving at 100°C resulted in a compressive strength of 21.8 MPa. This value markedly rose by nearly 2.5 fold when the autoclave temperature was increased to 200°C. A further increase in temperature to 300°C caused the retrogression of its strength; in fact, the value of 31.8 MPa was 41 % lower than of the 200°C-autoclaved cement. As described in our previous paper [1], the increase in strength at 200°C was due to the formation of well-crystallized calcium silicate hydrate (CSH) and tobermorite phases that further densify the cement's structure. However, at 300°C, two factors, the *in-situ* tobermorite → xonotlite phase transition and the overgrowths of tobermorite and xonotlite crystals in the cement bodies, were detrimental to retaining an ideal dense microstructure of cement, and consequently, were reflected in its conversion into a porous microstructure.

When the 10wt% of slag was replaced by MQMB, the features of the strength-temperature curve differed from that control cement; namely, the strength of the 90/10 ratio cement monotonously increased with higher autoclave temperatures. There was no sign in the curve of any striking increase in strength at 200°C. The value of 39.7 MPa developed at 300°C corresponded to an improvement of ~1.4- and ~2.7- fold, respectively, over those of 200°-and 100°C- autoclaved ones. Interestingly, the 300°C-autoclaved cement was even stronger than that of the control cement autoclaved at the same temperature. Features similar to the curve of the 90/10 ratio cement were observed in the 70/30 and 50/50 ratio cements. The data also revealed that incorporating the MQMB into slag retarded the development of strength. Correspondingly, the strength of the 70/30 ratio cements at 100°, 200°, and 300°C was ~49, ~41, and ~38% lower than

those of the 90/10 ratio at these each temperature. A further reduction in strength can be seen in the 50/50 ratio cement made by replacing more of slag with MQMB.

Nevertheless, these values of compressive strength for all the cements, except for that made with the 50/50 ratio at 100°C, met the strength criteria of more than 6.89 MPa.

### Water Permeability

The geothermal well cementing materials not only support mechanically the steel casing pipes, but also they must protect the pipes against the corrosion from the hot brine. Thus, one important property of the cements was their ability to minimize the extent of water permeability. Figure 2 plots the water permeability of the MQMB-modified and unmodified SSAS cements versus autoclave temperatures. At 100°C, water permeability depended mainly on the slag/ MQMB ratios; a decrease in the proportion of slag to MQMB enhanced permeability. In fact, the  $9 \times 10^{-3}$  Darcys of the 50/50 ratio cement was more than one order of magnitude higher than that of the unmodified (100/0 ratio) cement. Since the extent of water transportation was related to the number of continuous pores present in the autoclaved cements [3,4], cement containing a large number of continuous pores would allow water to permeate easily through it. Hence, a significant number of continuous pores appear to exist in the 100°C-autoclaved 50/50 ratio cement. After autoclaving at 200°C, water permeability decreased, probably reflecting a decline in the number of pores. A continuing drop in permeability was observed from all the MQMB-modified cements autoclaved at 300°C; it fell as low as  $10^{-5}$  Darcys level. In contrast, the water permeability of 300°C-autoclaved unmodified cement increased by nearly one order of magnitude compared with that of the 200°C one, suggesting that the overgrowths of tobermorite and xonotlite crystals in the cement bodies not only caused the development of a porous microstructure, but also appeared to have created numerous continuous pores.

### Resistance to Acid

Figure 3 depicts the changes in weight of the 100/0, 90/10, 70/30, and 50/50 ratio cements autoclaved at 100°, 200°, and 300°C after exposure for 15 days in a 90°C CO<sub>2</sub>-laden H<sub>2</sub>SO<sub>4</sub> solution. In this test, before measuring the cements' weights, we scoured off

any  $\text{H}_2\text{SO}_4$ -associated reaction products that had deposited on their outermost surfaces during exposure by brushing them well. For the unmodified cements, the loss in weight due to acid erosion was associated directly with the autoclave's temperature; loss increased with an increasing temperature. As much as 29.1 % weight loss was measured from the 300°C-autoclave cement. This value was tantamount to an increase of 44 % over that of the 100°C-autoclaved one. A similar increase in weight loss as a function of temperature occurred in the 90/10 ratio cement. However, their weight losses at each temperature were much lower than those of the 100/0 ratio cements. The 70/30 and 50/50 ratio cements autoclaved at those temperatures showed the lowest changes in weight, ranging from - 1.9 to + 1.3; interestingly, here the weight change-temperature relation showed that their weight losses tend to decrease with an increasing temperature. This finding strongly demonstrated that adding more MQMB was responsible for enhancing the SSAS cement's resistance to acid.

Based upon this information, we next concentrated on identifying the phase compositions assembled in the 70/30 ratio cement before and after exposure in acid, and also on exploring the microstructure and chemistry of the exposed cement's surface. These data would provide us with important information needed for explaining why this ratio cement displayed an outstanding resistance to acid. No further study was made of any other ratio cements.

#### Phase Identification of Unexposed and Exposed Cements

Figure 4 illustrates the XRD patterns, ranging from 0.225 to 0.444 nm, for the 100°C-, 200°C-, and 300°C-autoclaved 70/30 ratio cements before exposure in acid. At 100°C, the XRD tracing indicated only quartz-related d-spacings that arose from the MQMB. There were no d-spacings of any crystalline hydrates as the hydrothermal reaction products of cement. Thus, we believe that the major phase of the cementitious structure formed at 100°C was essentially amorphous, and it would bind together most of the partially reacted and non-reacted slag and MQMB particles into a cohesive mass, thereby developing some strength of the cement. Exposure to 200°C led to the formation of analcime ( $\text{NaAlSi}_2\text{O}_6 \cdot \text{H}_2\text{O}$ ) crystals of the zeolitic mineral family, while the line intensity of the quartz-related d-spacings declined. Since there were no d-spacings of

mullite ( $3\text{Al}_2\text{O}_3 \cdot 2\text{SiO}_2$ ) reactant in the MQMB, it is reasonable to assume that analcime was formed by interactions between the mullite and Na dissociated from the sodium silicate activator. One important effect of the crystalline analcime formed in the cement bodies was to improve their compressive strength compared with that of the amorphous phase-associated cement. At  $300^\circ\text{C}$ , a new reaction product, calcium silicate hydrate (I) [CSH(I),  $\text{CaO} \cdot \text{SiO}_2 \cdot x\text{H}_2\text{O}$ ] phase, was incorporated into the analcime phase. As seen in this XRD pattern, two factors, the prominent line intensity of CSH and the striking decay of quartz's line intensity, can be taken as evidence indicating that quartz favorably reacted with the sodium silicate-activated slag to assemble the well-formed CSH phase at this hydrothermal temperature.

Relating this finding to the results from the acid exposure tests, we found that the combination of the CSH and analcime phases played a pivotal role in abating significantly the vulnerability of cement to acid attack. To understand the specific roles of these phases in protecting the cement against acid erosion, we analyzed by XRD the samples collected by scrubbing away a layer approximately 1-mm in depth from the surfaces of  $300^\circ\text{C}$ -autoclaved 70/30 ratio cement after 15 days exposure. Figure 5 shows the XRD tracing of this sample. It revealed that this top layer encompassed three crystalline phases; bassanite ( $\text{CaSO}_4 \cdot 1/2\text{H}_2\text{O}$ ), analcime, and lizardite [ $\text{Mg}_2\text{Si}_2\text{O}_5(\text{OH})_4$ ]. No CSH-related d-spacings were detected in its XRD pattern, suggesting that the CSH phase in  $\sim 1$  mm thick superficial layer underwent the reactions with  $\text{H}_2\text{SO}_4$ , generating two  $\text{H}_2\text{SO}_4$ -induced corrosion products, bassanite and ionized monosilicic acid;  $\text{CaO} \cdot \text{SiO}_2 \cdot x\text{H}_2\text{O} + \text{H}_2\text{SO}_4 \rightarrow \text{CaSO}_4 \cdot 1/2\text{H}_2\text{O} + (\text{H}_2\text{SiO}_4)^{2-}$ , that were reflected in the absence of Ca in the CSH after acid exposure. On the other hand, the lizardite as magnesium silicate hydrate was formed spontaneously by reactions between the ionized monosilicic acid as a corrosion product of CSH and the Mg ions liberated from the activated slag;  $2(\text{H}_2\text{SiO}_4)^{2-} + 2\text{Mg}^{2+} + \text{H}_2\text{O} \rightarrow \text{Mg}_2\text{Si}_2\text{O}_5(\text{OH})_4 + 2\text{H}^+$ . Assuming that this reaction pathway is valid, the formation of lizardite not only restrains further acid erosion of the cement, but also shores up the damaged cementitious structure, thereby preserving its required mechanical and physical properties. Thus, the specific role of Mg in the slag was to promote self-healing of the damages that the MQMB-modified SSAS cement incurred from acid attack. Without the Mg, the ionized monosilicic acid would be leached

out from the cement during the exposure, leaving an undesirable porous structure that advances the penetration of acid through the cement and accelerates its acid erosion. The presence of analcime demonstrated that its susceptibility to reactions with  $H_2SO_4$  was a very little, if any, and also manifesting that analcime was among the factors governing the resistance to acid of the cement.

To support this information, we explored the surfaces of the same exposed cement as that used in XRD by EDX coupled with SEM (Figure 6). The SEM image revealed the typical microstructure representing the  $H_2SO_4$  attack on the cement's surface; namely, the surfaces were covered with a porous bassanite layer as the corrosion product of cement. The EDX spectrum taken from the area in the square had one pronounced elemental signal arose from Si, three moderate signals related to Ca, S, and Mg, and three weak signals from Al, Na, and O. Relating this data to the earlier XRD results, the first three elements, Ca, S, and O, were associated with bassanite, and the other three elements, Na, Al, and Si, in conjunction with O, were attributed to analcime, while lizardite related to Mg, Si, and O. Since the maximum penetration depth of the x-rays excited from EDX is  $\sim 2 \mu m$ , a superficial layer of  $\sim 2 \mu m$  thick on the exposed cement appears to be occupied by the hybrid phases involving bassanite, analcime, and lizardite, strongly underscoring that both the analcime and lizardite phases acted to alleviate an extensive formation of bassanite corrosion product.

## Conclusions

The manufactured quartz/mullite blend (MQMB) ceramic powder not only had high potential as an additive conferring substantial resistance to acid of the sodium silicate-activated slag (SSAS) cement, but also we recommended it for replacing Class F fly ash in the cement. The most effective MQMB-modified SSAS cement in mitigating the acid erosion in a  $90^\circ C$   $CO_2$ -laden  $H_2SO_4$  solution (pH 1.1) was made from the slag/MQMB ratio of 70/30; its effect was reflected in a loss in weight of less than 2 % after 15 days exposure. The phase composition assembled in this cement before exposure in acid differed with the temperature of autoclave, from  $100^\circ C$  to  $300^\circ C$ . The  $100^\circ C$ -autoclaved cement was comprised of essentially amorphous phases exhibiting the development of low compressive strength. At  $200^\circ C$ , crystalline analcime ( $NaAlSi_2O_6 \cdot H_2O$ ) of the

zeolitic mineral family was incorporated into the amorphous phases. Hydrothermal reactions between the mullite in MQMB and the Na dissociated from sodium silicate activator at this temperature led to the formation of analcime. Increasing the temperature to 300°C led to the appearance of the crystalline calcium silicate hydrate (I) (CSH) phase that was responsible for strengthening the cement. The CSH was formed by interactions between the activated slag and the quartz in MQMB. These two crystalline phases formed in the cement bodies, analcime and CSH, densified the cementitious structure, minimizing water permeability at  $10^{-4}$  Darcy level.

Correspondingly, the cement autoclaved at 300°C showed better performance in resisting acid than that of 100°C- autoclaved one. The reason for this was due to the creation of a new lizardite [ $\text{Mg}_2\text{Si}_2\text{O}_5(\text{OH})_4$ ] crystal phase coexisting with the analcime phase. Lizardite (magnesium silicate hydrate) was yielded by reactions between the Ca-depleted CSH brought about by acid attack and Mg liberated from activated slag. Without the Mg, the ionic monosilicic acid,  $(\text{H}_2\text{SiO}_4)^{2-}$ , derived from the Ca-depleted CSH, would be leached out from the cement during the acid exposure, resulting in an undesirable porous structure and accelerating its acid erosion. Thus, a specific role of Mg was to promote the self-healing activity of MQMB-modified SSAS cement, which had been damaged by exposure to acid. On the other hand, the susceptibility of analcime to reactions with  $\text{H}_2\text{SO}_4$  was a very little, if any, denoting that analcime was among the factors governing the resistance to acid of the MQMB-modified SSAS cement.

## References

1. T. Sugama and L.E. Brothers, "Sodium-silicate-activated slag for acid-resistant geothermal well cements", Advances in Cement Research, 16, (2004) 77-87.
2. T. Sugama, L.E. Brothers, and T.R. Van de Putte, "Acid-resistant cements for geothermal well: Sodium silicate-activated slag/fly ash blends", Advances in Cement Research, (in press).
3. Tonyan, T.D. & Gibson, L.J., Structure and mechanics of cement foams. *J. Mater. Sci.* 27 (1992) 6371-6378.
4. Hoff, G.C., Porosity-strength considerations for cellular concrete. *Cem. Conc. Res.* 2 (1972) 91-100.

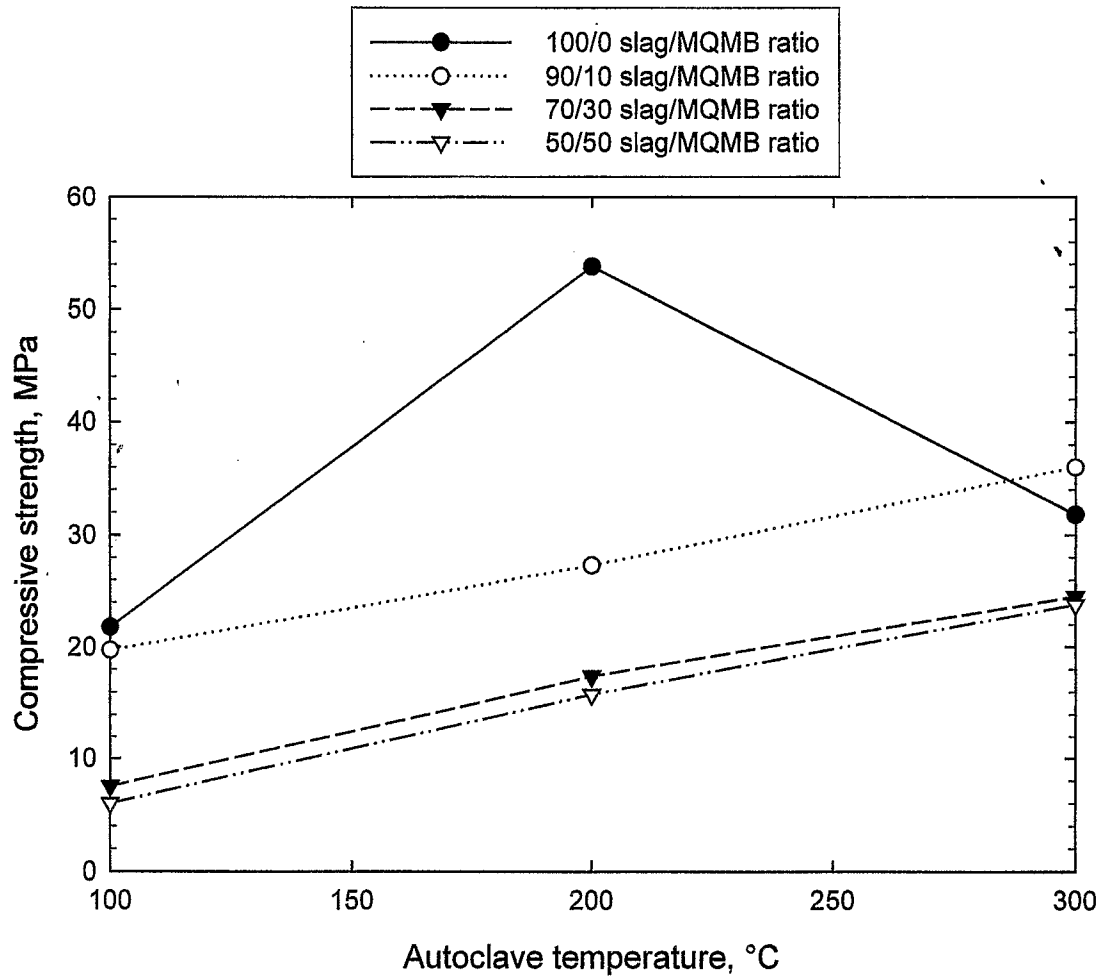


Figure 1. Compressive strength versus autoclave temperature for 100/0, 90/10, 70/30, and 50/50 slag/MQMB ratio cements.

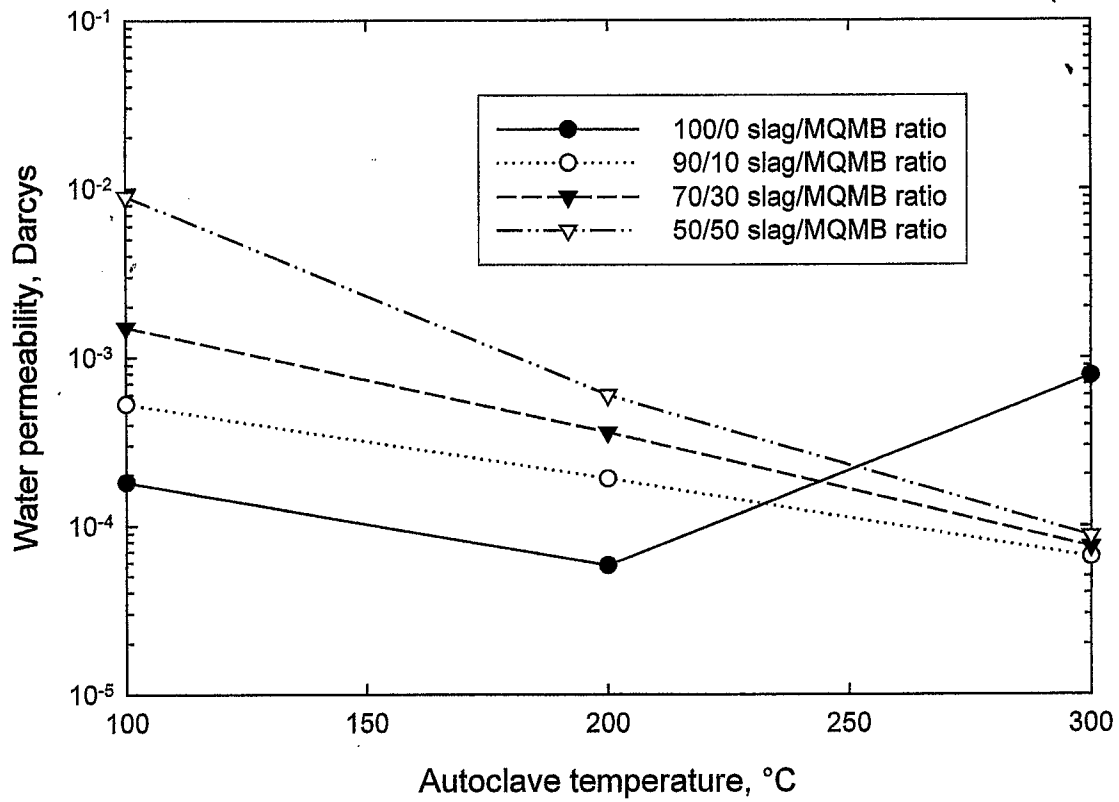


Figure 2. Changes in water permeability of the cements made with various slag/MQMB ratios as a function of autoclave temperature.

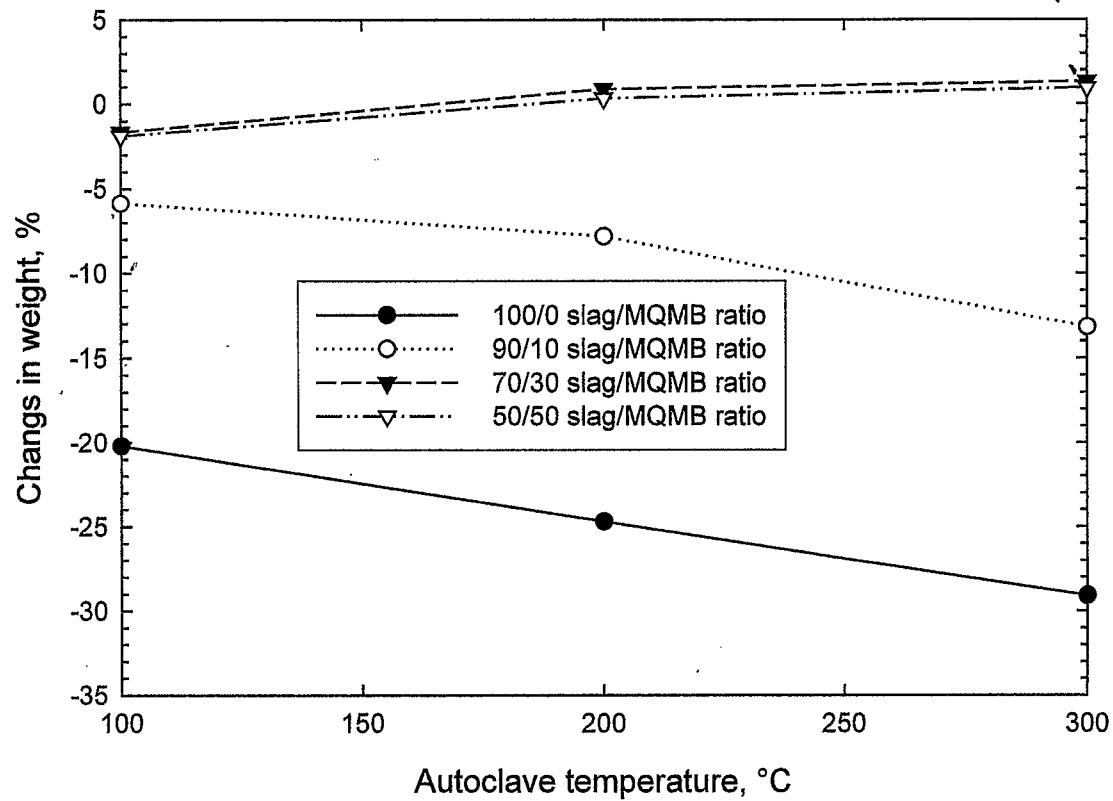


Figure 3. Changes in weight of various slag/MQMB ratio cements autoclaved at 100°, 200°, and 300°C after exposure in 90°C CO<sub>2</sub>-laden H<sub>2</sub>SO<sub>4</sub> solution (pH 1.1) for 15 days.

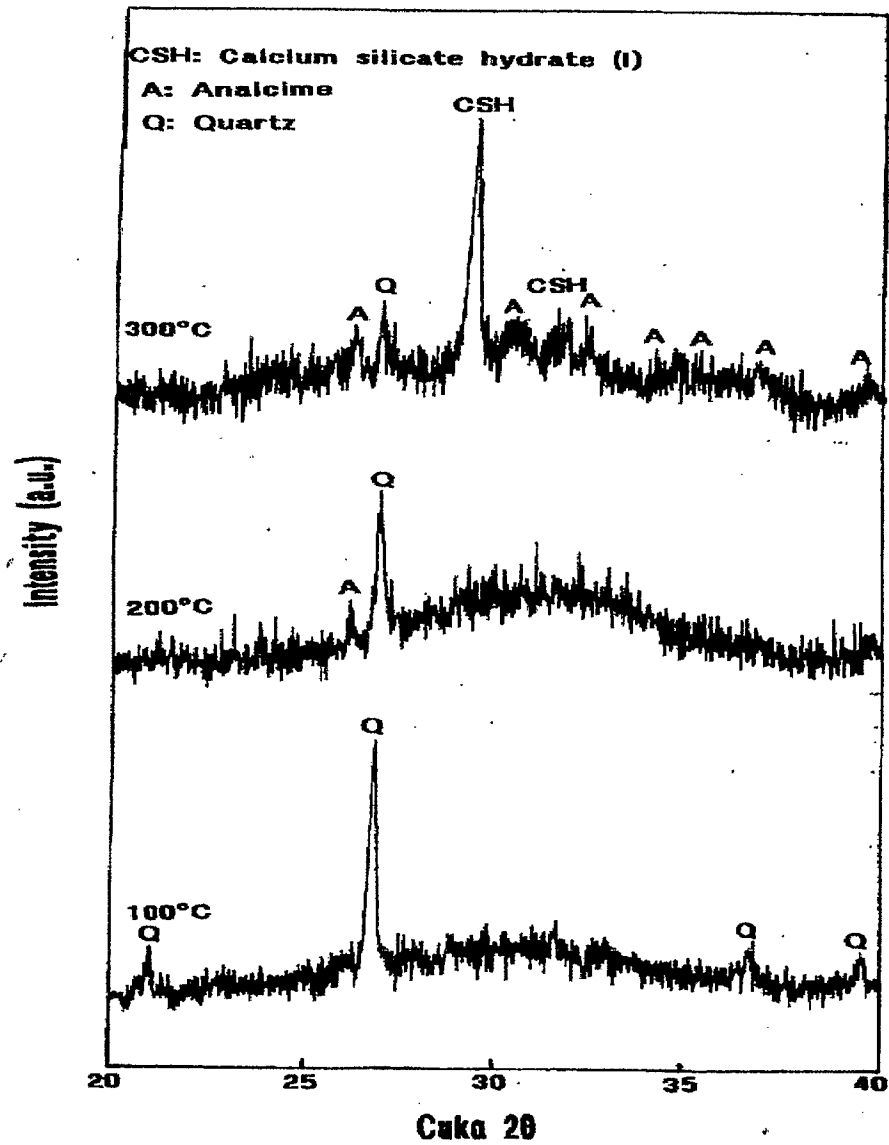


Figure 4. XRD patterns for 100°C-, 200°C-, and 300°C-autoclaved 70/30 ratio cements.

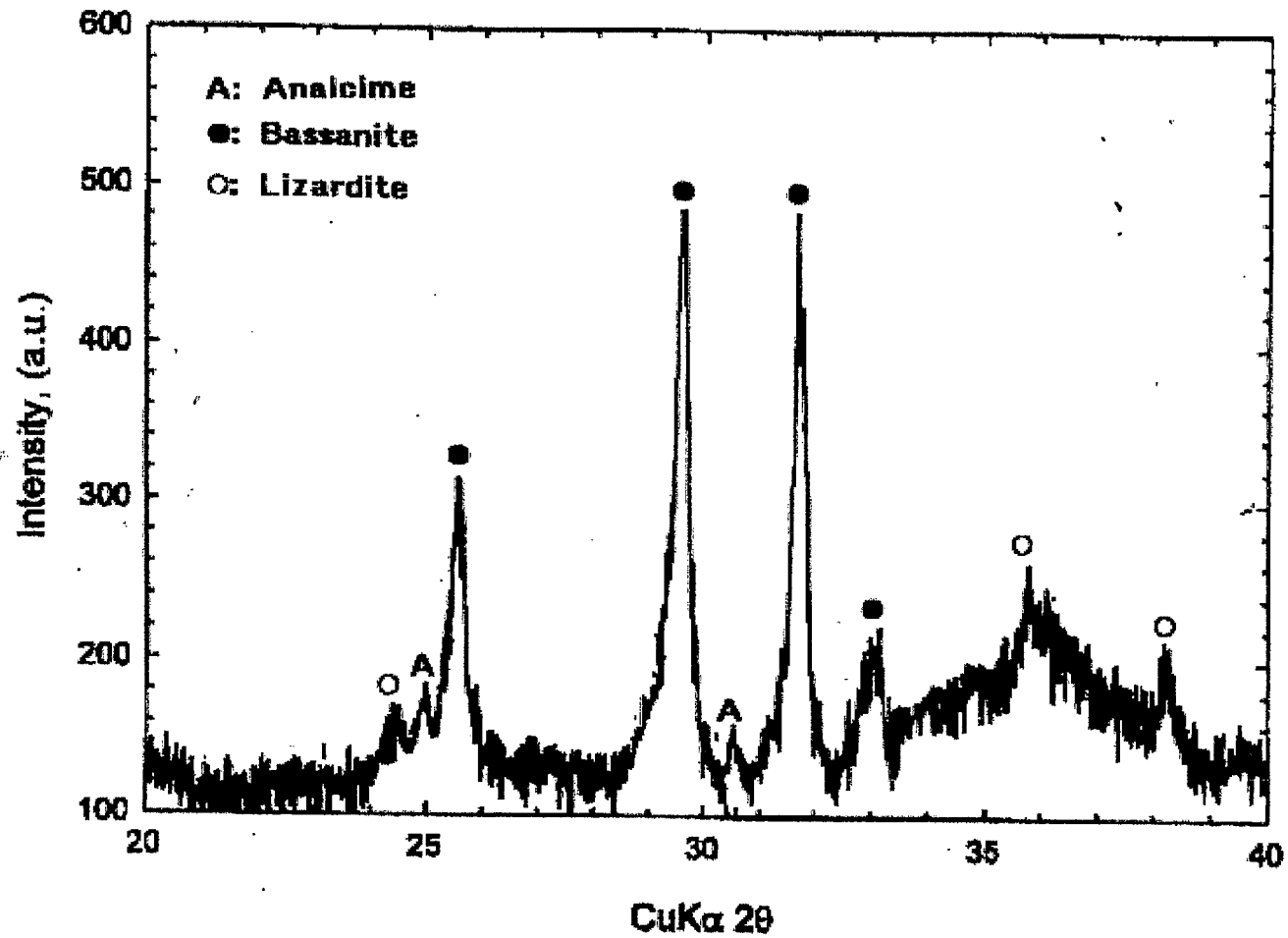


Figure 5. XRD tracing for the sample collected from the surface of 70/30 ratio cement after 15 days exposure.

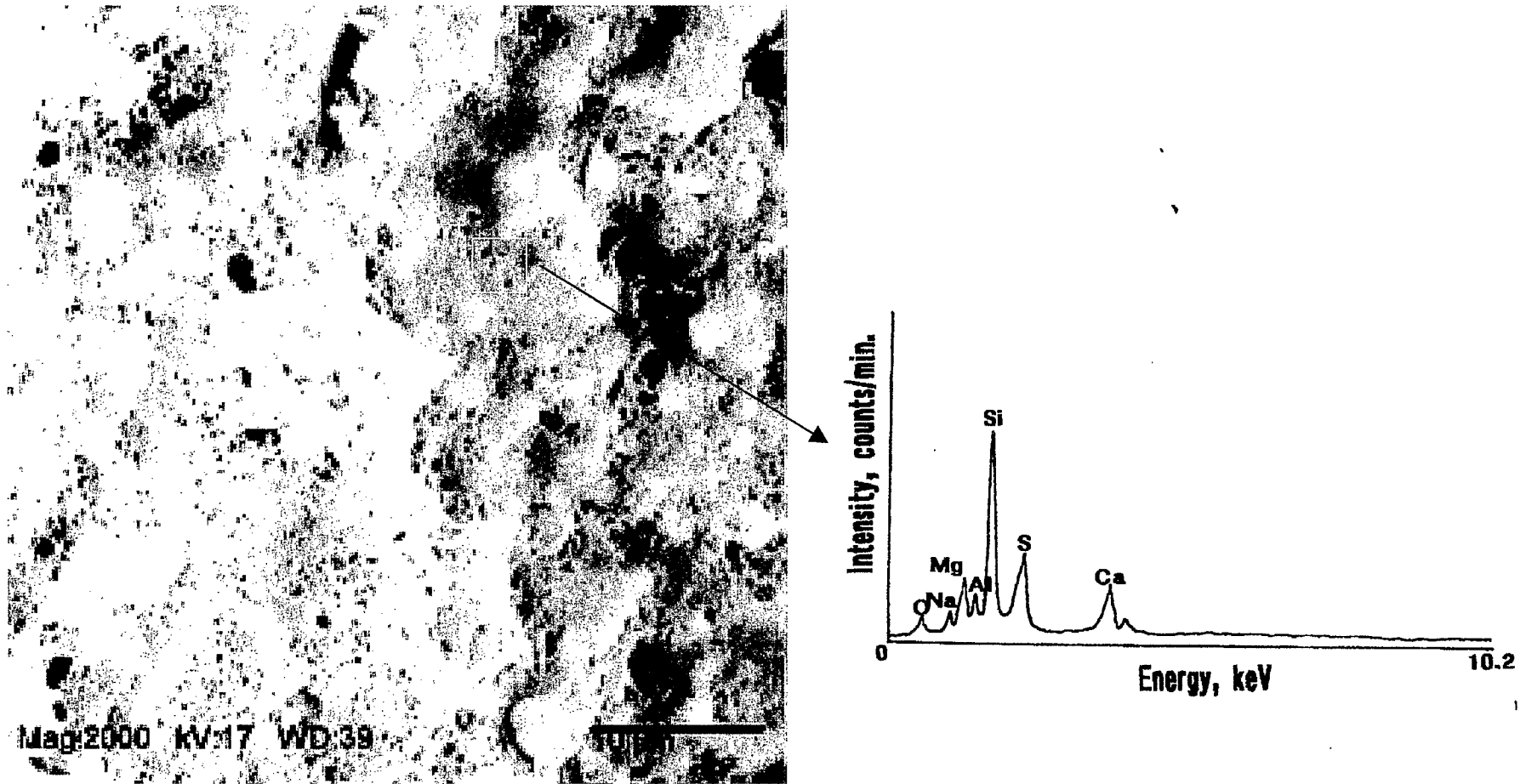


Figure 6. SEM image coupled with EDX spectrum for the surface of exposed 70/30 ratio cement.